International Journal of Innovation and Industrial Revolution
IJIREV
EISSN: 2637-0972
Volume 7 Issue 20 (March 2025) PP. 352-369
DOI 10.35631/IJIREV.720023

INTERNATIONAL JOURNAL OF INNOVATION AND INDUSTRIAL REVOLUTION (IJIREV)
www.ijirev.com

GLOBAL ACADEMIC EXCELLENCE

RADIATION SHIELDING PROPERTIES OF TIN-POLYDIMETHYLSILOXANE (PDMS) COMPOSITES AGAINST GAMMA RAY AT 356 KEV

Hanisah Zainal Abidin[1], Nur Maizatul Azra Mukhtar[2*], Ainorkhilah Mahmood[3], Nor Aimi Abdul Wahab[4], Rafidah Zainon[5], Nurul Syafiqah Roslan[6]

[1] Department of Applied Sciences, Universiti Teknologi MARA Cawangan Pulau Pinang, 13500 Permatang Pauh, Pulau Pinang, Malaysia
Email: 2023650308@student.uitm.edu.my
[2] Faculty of Health Sciences, Universiti Teknologi MARA Cawangan Pulau Pinang, 13200 Kepala Batas, Pulau Pinang, Malaysia
Email: nurmaizatul038@uitm.edu.my
[3] Department of Applied Sciences, Universiti Teknologi MARA Cawangan Pulau Pinang, 13500 Permatang Pauh, Pulau Pinang, Malaysia
Email: ainorkhilah_sp@uitm.edu.my
[4] Department of Applied Sciences, Universiti Teknologi MARA Cawangan Pulau Pinang, 13500 Permatang Pauh, Pulau Pinang, Malaysia
Email: noraimi108@uitm.edu.my
[5] Department of Biomedical Imaging, Advanced Medical and Dental Institute, Universiti Sains Malaysia, SAINS@BERTAM, 13200 Kepala Batas, Pulau Pinang, Malaysia
Email: rafidahzainon@usm.my
[6] Department of Applied Sciences, Universiti Teknologi MARA Cawangan Pulau Pinang, 13500 Permatang Pauh, Pulau Pinang, Malaysia
Email: 2024592857@student.uitm.edu.my
[*] Corresponding Author

Article Info:

Article History:
Received date: 29.01.2025
Revised date: 17.02.2025
Accepted date: 20.03.2025
Published date: 30.03.2025

To Cite This Document:

Zainal Abidin, H., Mukhtar, N. M. A., Mahmood, A., Abdul Wahab, N. A., Zainon, R., & Roslan, N. S. (2025).

Abstract:

Radiation shielding materials are essential for various applications, but conventional lead-based (Pb) shields pose environmental and health risks. This study investigates polydimethylsiloxane (PDMS) reinforced with tin as a sustainable alternative. Composites with varying tin concentrations were fabricated and analysed using Fourier Transform Infrared Spectroscopy (FTIR) and Field Emission Scanning Electron Microscopy (FESEM) to evaluate structural integrity and morphology. Shielding performance was assessed through Mass Attenuation Coefficient (MAC), Half-Value Layer (HVL), and Radiation Protection Efficiency (RPE). The results indicate that increasing tin content improves attenuation performance. Composites with 50% and 60% tin filler exhibited the highest MAC values (0.0905 and 0.0762

International Journal of Innovation and Industrial Revolution
EISSN: 2637-0972
Volume 7 Issue 20 (March 2025) PP. 352-369
DOI 10.35631/IJIREV.720023

Radiation Shielding Properties Of Tin-Polydimethylsiloxane (PDMS) Composites Against Gamma Ray At 356 KEV. *International Journal Of Innovation And Industrial Revolution, 7* (20), 352-369.

DOI: 10.35631/IJIREV.720023

$cm^2\ g^{-1}$) and RPE (16.26 and 16.89 %) while maintaining lower HVL (1.91 and 2.02 cm), respectively, making them the most promising candidates. Although control lead showed the highest MAC, Pb toxicity remains a major concern, reinforcing the need for alternative materials. FTIR analysis confirmed successful interaction between tin and PDMS, while FESEM images showed uniform tin dispersion at optimal concentrations. However, higher tin loading resulted in agglomeration, potentially affecting performance. Control PDMS exhibited the lowest efficiency, confirming its limited attenuation capability. Tin-reinforced composites demonstrated enhanced shielding due to tin's high atomic number, increasing photon interactions. While HVL variations were observed, results suggest that an optimal tin concentration is necessary to achieve efficient shielding without compromising mechanical stability. In conclusion, tin-reinforced PDMS composites show strong potential as lead-free shielding materials with competitive attenuation properties. Their improved performance, combined with environmental and health benefits, supports their feasibility for radiation protection. Future work should focus on optimising tin dispersion and evaluating long-term durability. These findings contribute to the advancement of sustainable, non-toxic materials for shielding applications.

Keywords:

Attenuation, Polydimethylsiloxane, Radiation, Shielding, Tin

Introduction

Gamma rays have short wavelengths, giving them high energy and power compared to other electromagnetic waves. They are widely used in cancer treatment through radiation therapy, which helps control or destroy malignant tumour cells. However, gamma rays can also harm healthy tissues, leading to organ damage (Ali, Cucinotta, Ning-Ang, & Zhou, 2020; Cioffi et al., 2020; Kochanova et al., 2023; Vaiserman, Koliada, Zabuga, & Socol, 2018). To minimise these risks, radiation shielding materials are essential for protecting patients and radiation workers (Boniface & Mukhtar, 2020; Kamarolzeman & Mukhtar, 2020; Mukhtar et al., 2024). With the increasing global shift towards nuclear technology for energy and medical applications, radiation protection has become a crucial concern. While lead remains the most commonly used shielding material, its toxicity and environmental impact have driven researchers to seek safer alternatives (M. El-Sharkawy, Abdou, Gizawy, Allam, & Mahmoud, 2023; Mehrara, Malekie, Kotahi, & Kashian, 2021; Wahyuni, Sakti, Herry Santjojo, & Juswono, 2022).

Traditional shielding materials include lead (Pb), cadmium (Cd), tin (Sn), and bismuth (Bi), all of which have high atomic numbers and excellent radiation-blocking properties (Asgari, Afarideh, Ghafoorifard, & Amirabadi, 2021; El-Khatib et al., 2019). However, these materials often lack flexibility, making them impractical for use in protective garments. In response, researchers have explored polymer-based composites as a more adaptable alternative. Polymers offer advantages such as low density, corrosion resistance, flexibility, and durability (Altan & Yavuz, 2016; Barabash, Barabash, Pertsev, & Panfilov, 2019). By incorporating high-Z materials like lead oxide (PbO) or bismuth oxide (Bi_2O_3) into polymer matrices, scientists aim to develop flexible, lightweight, and efficient radiation shielding materials (Bijanu et al., 2021; Rajendran et al., 2023).

Elastomeric materials such as PDMS provide an innovative solution for flexible radiation shielding. Unlike rigid shielding materials, PDMS-based composites can be moulded into different shapes, making them suitable for wearable protection. Several research groups have developed polymer-based radiation shields by incorporating nanofillers like lead oxide, bismuth oxide, and tungsten-based compounds (Alresheedi et al., 2023a, 2023b; Wang et al., 2021). These materials have shown promising results in enhancing shielding efficiency while maintaining flexibility and lightweight properties.

The study by Abualroos et al. reported that the composites of lead mixed with epoxy resin showed enhanced properties in shielding materials at low energy gamma rays (60 keV). The study also stated that a polymer and metal with high density produced an improved composite for radiation shielding (Abualroos, Idris, Ibrahim, Kamaruzaman, & Zainon, 2024). Besides, the study from El Sharkawy mentioned that as the energy of gamma rays increases, the MAC decreases due to the changes in photon interactions and energy behaviour. The study also includes the findings describing the increase in MAC as the concentration of metal filler increased (bismuth oxide) (M. El-Sharkawy et al., 2023). From the studies, the hypothesis that could be generated is that the highest concentration of metal filler can provide enhanced shielding properties. However, this also depends on the radiation energies used and the density of the materials used.

Therefore, this study focuses on developing a flexible gamma-ray shielding material using PDMS as the polymer matrix, embedded with different weight fractions of tin powder by analysing their structural, chemical and radiation attenuation performance. Characterisation technique using FESEM was used to analyse particle size and distribution. The chemical bonding and characteristics were assessed using FTIR. The composite was tested against the moderate energy of a gamma-ray source (Ba-133). The shielding performance of microscale tin fillers was compared to assess the material's effectiveness in radiation shielding attenuation. By optimising the composition and processing conditions, the goal is to develop a non-toxic, flexible, and efficient radiation shielding material suitable for medical, industrial, and nuclear applications.

Theory

The incoming photon rays will either pass through or be absorbed by the blocking material when they contact it. The type of material itself affects the interaction in the material depending on the energy levels. When photon beams interact inelastically with materials, three (3) distinct processes occur such as pair production, Compton scattering, and the photoelectric effect. At low photon energy levels, usually between 10 and 100 keV, the photoelectric effect takes place. An electron is ejected when the inner-shell electron absorbs an incoming photon with more energy than the core electron. For the ejected photoelectron, the remaining electron is converted into kinetic energy. This method is important for materials like lead, bismuth, and tungsten that have high Z shielding and low photon energy (Bijanu et al., 2021; Kaur, Sharma, & Singh, 2019; Mollah, 2019; Zhang et al., 2021).

In the energy range of 100 keV to 10 MeV, Compton scattering also known as inelastic scattering dominates. A photon and an outer-shell electron collide in this interaction, reducing the photon's energy or wavelength and changing its direction. The electron has less energy than the incident photon. By scattering photon beams in multiple directions, this interaction further reduces radiation intensity. It is more likely that the lower-energy scattered photons will be

International Journal of Innovation and Industrial Revolution
EISSN: 2637-0972
IJIREV
Volume 7 Issue 20 (March 2025) PP. 352-369
DOI 10.35631/IJIREV.720023
absorbed by the shielding material (Aim-O, Wongsawaeng, Phruksarojanakun, & Tancharakorn, 2017; Bijanu et al., 2021; Kaur et al., 2019; Mollah, 2019).

In contrast, pair creation absorbs and removes energy from a photon to create an electron-positron pair. When an electron is destroyed by the positron, two (2) gamma-ray photons are released. Incoming photons in this interaction need to be twice as powerful as the rest mass (0.511 MeV). The intensity of photon radiation will ultimately decrease as a result of these annihilation photons' ongoing interactions with shielding materials. Throughout the shielding process, high-energy gamma rays may continuously experience pair production interaction or Compton scattering as the intensity is reduced, and the gamma-ray may be absorbed by the materials (Bijanu et al., 2021; Kaur et al., 2019; Mollah, 2019; Pianpanit & Saenboonruang, 2022).

Quantifying the shielding effectiveness of materials is essential in radiation protection studies. The capability of composites to attenuate photon rays involves the examination of linear attenuation coefficients (LAC), MAC, Half Value Layer (HVL), and RPE. The intricate relationship can be computed for RPE, representing the composite's ability to block photon ray intensity, by considering density, and thickness, and expressing it through equations (i) and (ii), which are formulated using intensity (Kilicoglu et al., 2022; Ozel et al., 2021):

$$RPE = (1 - e^{-\mu x}) \times 100 \tag{i}$$

$$RPE = \left(1 - \frac{I}{I_O}\right) \times 100 \tag{ii}$$

Where I is the intensity of the transmitted ray, I_o is the intensity of the incident ray, μ is LAC of the sample and x is the thickness of the sample.

The HVL signifies the thickness of the composite needed to halve the intensity. A higher HVL value suggests lower effectiveness in attenuating radiation, indicating the requirement for a thicker layer for adequate protection. HVL can be calculated using the LAC of the composite, as seen in equation (iii). The tenth-value layer (TVL) in equation (iv) is the material thickness needed to reduce radiation to 10%, while the mean free path (MFP) in equation (v) is the average distance a photon travels before interaction (Alshahri et al., 2021; Ersoz, Lambrecht, & Soylu, 2016; Kawady, Elkattan, Salah, & Galhoum, 2022; M. El-Sharkawy et al., 2023; Pianpanit & Saenboonruang, 2022):

$$HVL = \frac{ln\,2}{\mu} \tag{iii}$$

$$TVL = \frac{\ln 10}{\mu} \tag{iv}$$

$$MFP = \frac{1}{\mu} \tag{v}$$

International Journal of Innovation and Industrial Revolution
EISSN: 2637-0972
IJIREV
Volume 7 Issue 20 (March 2025) PP. 352-369
DOI 10.35631/IJIREV.720023

Equations (vi), (vii), and (viii) related to Lambert's Beer Law can be used to calculate the intensity of transmitted gamma rays after they have passed through a composite. The possibility of interactions with material, including scattering and absorption, rises with the degree of photon ray penetration. Greater thickness reduces the intensity of transmitted radiation because it increases the probability that photons may be scattered or absorbed (Aladailah et al., 2022; Yılmaz, Güngör, & Özdemir, 2020):

$$I = I_0 \mathrm{e}^{-\mu l x} \tag{vi}$$

$$\mu_m = \frac{\mu}{\rho} = \sum_i w_i \left(\frac{\mu_i}{\rho_i}\right) \tag{vii}$$

$$\mu_m = \left(\frac{\mu}{\rho}\right) = \frac{1}{\rho x} ln \frac{I_0}{I} \tag{viii}$$

Where μ_i is the linear attenuation coefficient of the sample at a specific gamma-ray, μ_m is MAC, ρ is density and w is weight fraction.

Materials and Method

Fabrication of The Composites

The composite was prepared by adding pure tin powder as filler at ratios of 10%, 20 %, 30 %, 40 %, 50 %, and 60 % metal into the PDMS (PDMS) matrix. The PDMS polymer functions as a binder to the tin powder. Table 1 shows the details of the raw material used. The pure tin powder of an average of 8 µm is purchased from Progressive Scientific Sdn. Bhd. While for the PDMS polymer liquid, the Sylgard Kit Set is purchased from HardwareMISE Sdn. Bhd. which consists of PDMS elastomer and PDMS curing agent. Table 2 shows the details for each composite.

Table 1 Material Properties of The Tin-PDMS Based Composites

Properties	Pure Tin	PDMS polymer
Symbol	Sn	C_2H_6OSi
Form	Powder	Liquid
Particle size (APS)	8 µm	-
Manufacturer/Supplier	Progressive Scientific Sdn. Bhd.	HardwareMISE Sdn. Bhd.
Density (g cm^{-3})	7.31	1.103
Liquid viscosity	-	3500 cP
Purity (%)	99.8	-
Melting point	231.9 °C	-

Throughout the composite preparation process, tin powder is weighed in the ceramic bowl and details for the composite's composition and density measured are given in Table 2. The curing agent and PDMS liquid were then added to the pure tin powder. Both ingredients were

International Journal of Innovation and Industrial Revolution
IJIREV
EISSN: 2637-0972
Volume 7 Issue 20 (March 2025) PP. 352-369
DOI 10.35631/IJIREV.720023
combined at the optimum speed to guarantee that the powder could be evenly dispersed throughout the polymer matrix. The mixture was poured into a 2.0 cm by 2.0 cm mould at 0.5 cm thick.

The composite was initially prepared and partially cured at room temperature before being cured in a dry oven at 100 °C for 35 minutes. The first curing step was completed in a glass vacuum desiccator to degas the air for about 30 minutes. Following oven curing, the sample was left to cool at room temperature for 30 minutes before being taken out of the mould and placed into the sealed container.

Table 2 The Details of The Tin/PDMS Composites

Composition of tin (%)	Label	Measured thickness (cm)	Calculated density (g cm^{-3})	Theoretical density (g cm^{-3})	Density deviation (%)
0	C	0.51	1.025	1.103	7.07
10	PT1	0.49	1.607	1.724	6.79
20	PT2	0.49	2.066	2.344	11.86
30	PT3	0.50	2.915	2.965	1.69
40	PT4	0.50	3.395	3.586	5.53
50	PT5	0.50	4.000	4.207	4.91
60	PT6	0.52	4.500	4.827	6.78

Structural Characterization

Using equipment provided by the Science & Engineering Research Centre (SERC), Usains Biomics Laboratory Testing Services Sdn Bhd, Universiti Sains Malaysia, a FESEM was used to examine the cross-sectional surface of the tin and PDMS hybrid polymer composites. The Everhart-Thornley Detector (ETD) (Secondary Electron), a beam current of 0.20 nA, and an accelerating voltage (HV) of 10.00 kV were used for the FESEM investigation. to minimise charging effects on sensitive or non-conductive materials and maximise resolution. A gold coating with copper tape was applied to the composite to allow for the measurement by FESEM effectively. The overview and the schematic image of the FESEM analysis are illustrated in Figure 1(a) and Figure 1(b).

International Journal of Innovation and Industrial Revolution
IJIREV
EISSN: 2637-0972
Volume 7 Issue 20 (March 2025) PP. 352-369
DOI 10.35631/IJIREV.720023

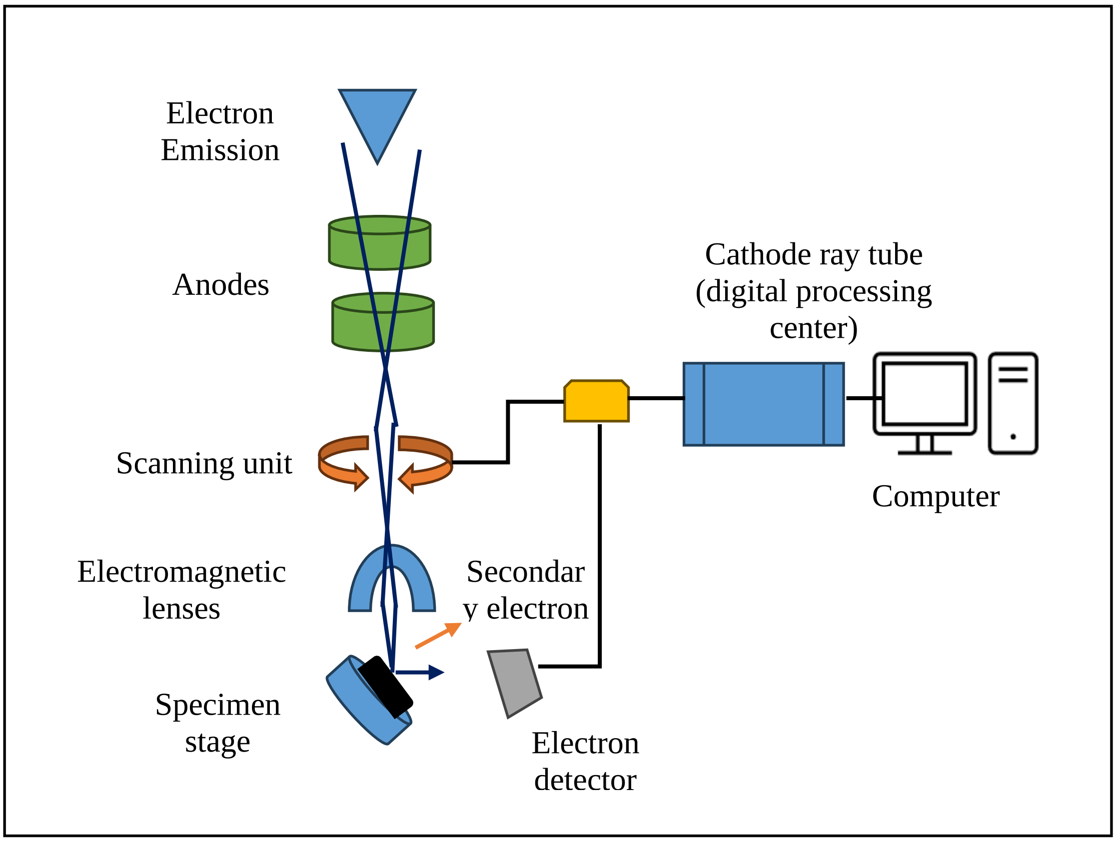

(a)

(b)

Figure 1: (a) Schematic Diagram of FESEM Process (b) FESEM Instrumentation at SERC

International Journal of Innovation and Industrial Revolution
IJIREV
EISSN: 2637-0972
Volume 7 Issue 20 (March 2025) PP. 352-369
DOI 10.35631/IJIREV.720023

Chemical Characterization

The FTIR (Figure 2(a) and Figure 2(b)) with the brand PerkinElmer model Spectrum 100 series with a 4000 - 400 cm^{-1} wavenumber were used to acquire molecular vibration data on samples at room temperature at Universiti Putra Malaysia (UPM).

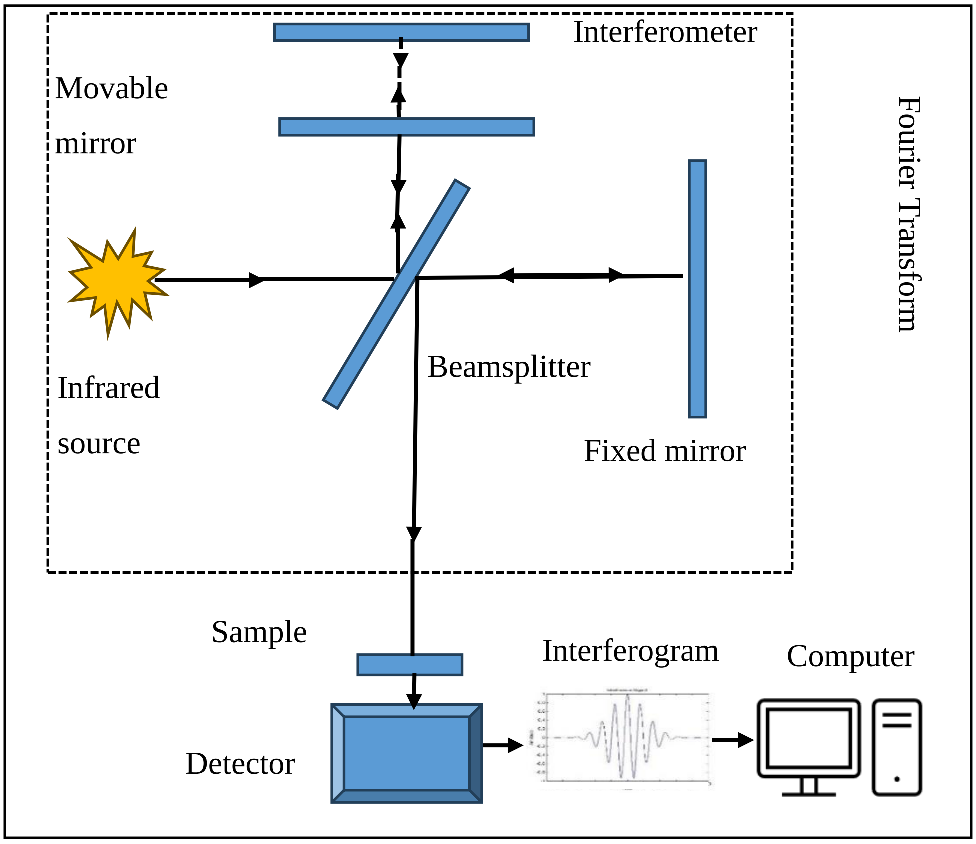

(a)

(b)

Figure 2: (a) Schematic Diagram of FTIR Analysis Process and (b) FTIR Instrumentation at UPM

International Journal of Innovation and Industrial Revolution
EISSN: 2637-0972
IJIREV
Volume 7 Issue 20 (March 2025) PP. 352-369
DOI 10.35631/IJIREV.720023

Radiation Characterization

Radiation characterization was carried out using gamma-ray spectroscopy. A high-precision detector, namely a NaI (TI) scintillation detector at Universiti Kebangsaan Malaysia (UKM). The detector is positioned at a predefined distance to quantify the intensity of radiation passing through the material, while a gamma-ray source of Barium-133 with 356 keV of energy level was set up in a controlled measurement setting. The PDMS/tin composites were placed between a gamma-ray source and a detector as illustrated in Figures 3(a) and 3(b).

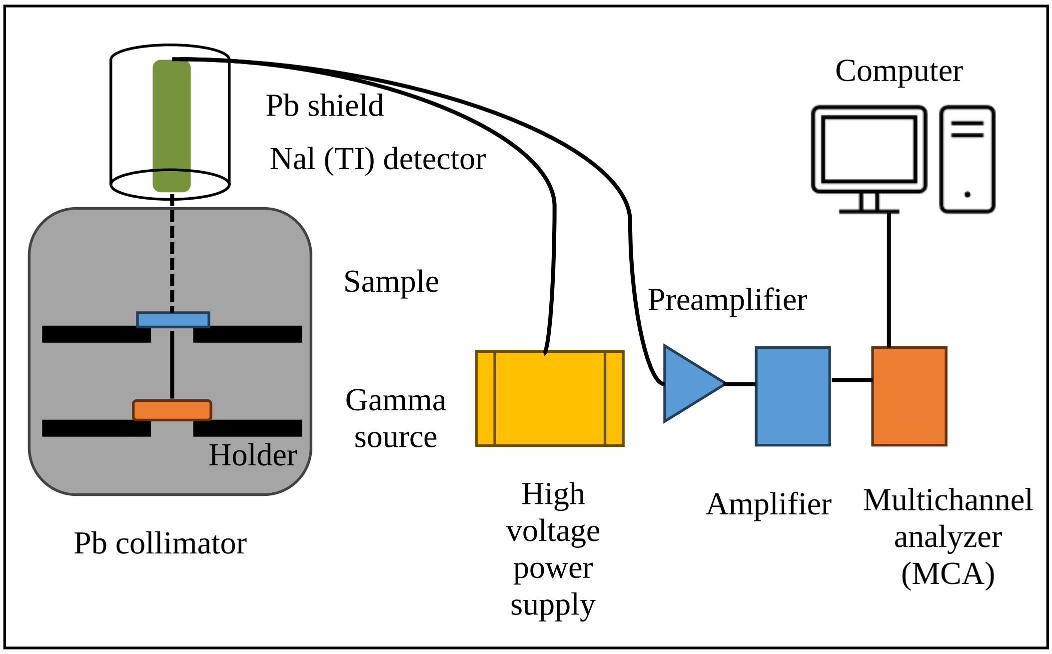

(a)

(b)

Figure 3: (a) Illustration of The Gamma-Ray Spectroscopy Set Up (b) Gamma-Ray Spectroscopy Instrumentation at Universiti Kebangsaan Malaysia (UKM)

International Journal of Innovation and Industrial Revolution
EISSN: 2637-0972
Volume 7 Issue 20 (March 2025) PP. 352-369
DOI 10.35631/IJIREV.720023

Result and Discussion

The cross-sectional FESEM image of the uniformly dispersed tin filler inside the PDMS matrixes is shown in Figure 4. FESEM study shows a diverse particle size distribution, with an average tin particle size of about 8 µm. This variety of particle sizes indicates that the tin powder utilized in the composite has a wide range of sizes. No particle separation or peeling from the PDMS matrix is observed. Strong tin-PDMS adhesion indicates good surface compatibility, which is essential for ensuring the composite's integrity. The tin particles' physical properties with the PDMS polymer showed improved bonding and even distribution throughout the matrix.

FESEM images also reveal an increase in the quantity of metal particles in the PDMS matrix in proportion to the metal composition. Additionally, there is no apparent agglomeration or crack within the composites, and the tin particles stay evenly distributed despite the rise in metal content. This suggests that even at larger tin compositions, the composite retains its structural stability, which is crucial for offering reliable shielding qualities (Bijanu et al., 2021; Zainal Abidin et al., 2025). The successful incorporation of tin particles into the PDMS matrix demonstrates the efficiency of the fabrication procedure and strengthens the potential of incorporating tin with PDMS in radiation shielding composites.

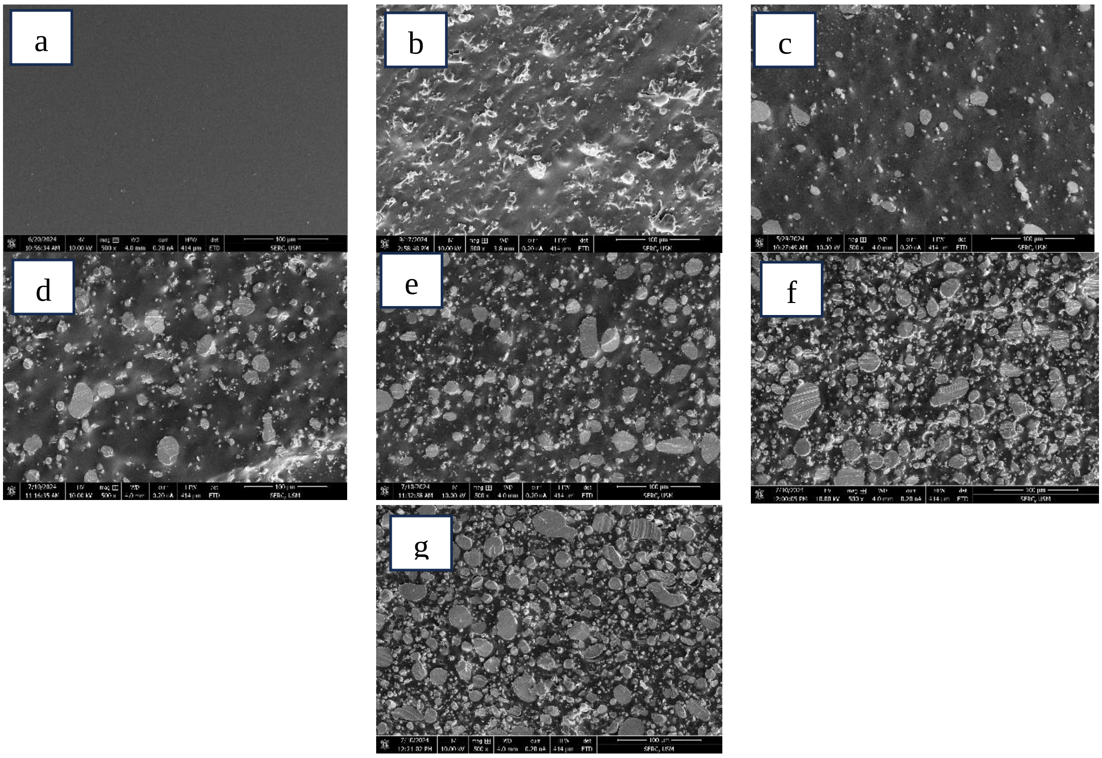

Figure 4: FESEM Images at 500 x Magnification of (a) C, (b) PT1, (c) PT2, (d) PT3, (e) PT4, (f) PT5 and (g) PT6

The transmittance patterns of the control and tin-reinforced PDMS composites are shown in the FTIR spectra over a range of wavenumbers in Figure 5. All samples exhibit key PDMS characteristic peaks, indicating that the polymer structure was retained following tin insertion. Si–O–Si stretching vibrations are represented by the peaks at 1000 to 1100 cm^{-1}, whereas C–H stretching from the polymer backbone is indicated by the absorption bands around 2900 cm^{-1}.

International Journal of Innovation and Industrial Revolution
IJIREV
EISSN: 2637-0972
Volume 7 Issue 20 (March 2025) PP. 352-369
DOI 10.35631/IJIREV.720023

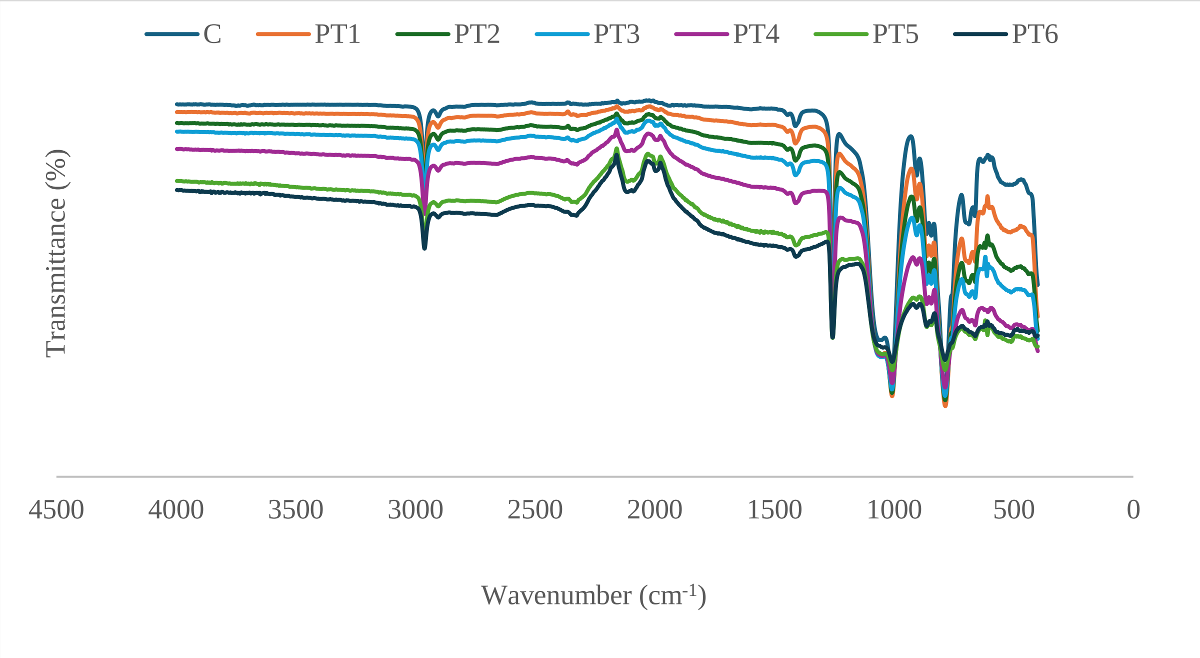

Figure 5: FTIR Spectra of C and Tin/PDMS Composites

Significant differences in transmittance intensity between PT1 and PT6 indicate modifications in molecular interactions brought on by an increase in tin concentration. The most noticeable alterations are seen in PT5 and PT6, which suggests that the tin particles and the PDMS matrix have a stronger link. These samples' lower transmittance might be a sign of increased filler dispersion or altered cross-linking between the PDMS matrix and tin filler, both of which could improve radiation attenuation and material stability. Additional peaks or peak shifts at lower wavenumbers indicate possible interactions between the functional groups of the polymer and tin, strengthening the composite's structural stability (Körpınar, Öztürk, Çam, & Akat, 2020; Ozel et al., 2021).

The observed spectral fluctuations demonstrate the influence of tin incorporation on the molecular properties of the composite, while the overall FTIR data verify that the basic PDMS structure is unaltered following reinforcement. These results support the potential benefits of adding tin to PDMS-based radiation shielding materials.

The characterization of radiation using gamma rays provides critical insights into the shielding performance of materials. Key parameters like the RPE, LAC, MAC, HVL, TVL, and MFP are commonly used to quantify the interaction between gamma rays and shielding materials (Abualroos et al., 2024; Gouda, Abbas, Hammoury, Zard, & El-Khatib, 2023). These parameters vary with the energy of the gamma rays, which significantly influences the shielding efficiency. Details for the radiation characteristics of the tin/PDMS are tabulated in Table 3 and the MAC and LAC values, which reveal the composites' effectiveness as shields is displayed in Figure 6.

International Journal of Innovation and Industrial Revolution
IJIREV
EISSN: 2637-0972
Volume 7 Issue 20 (March 2025) PP. 352-369
DOI 10.35631/IJIREV.720023

Table 3: MAC and LAC Properties of Tin/PDMS Composites at 356 KeV Energy Level

Composite	MAC ($cm^2\ g^{-1}$)	LAC (cm^{-1})
C	0.2416	0.2477
CL	0.2377	2.6951
CT	0.0916	0.6680
PT1	0.0470	0.0754
PT2	0.0418	0.0864
PT3	0.0496	0.1445
PT4	0.0607	0.2062
PT5	0.0905	0.3622
PT6	0.0762	0.3427

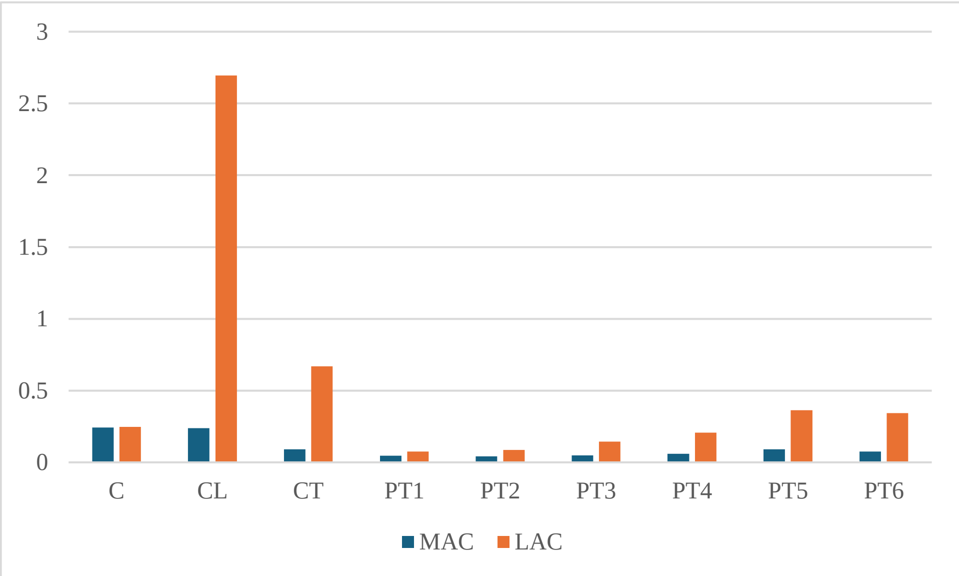

Figure 6: MAC and LAC Values of C, Control Lead 99.99% (CL), Control Tin 99.99% (CT) and Tin/PDMS (PT) Composites at 356 KeV Energy Level

The higher the MAC value or LAC value, the more absorption occurs in shielding material and less penetration of gamma rays. Since pure PDMS has a low density, it has weak radiation attenuation. C has the lowest LAC at 0.2477 cm^{-1} and the highest MAC of 0.2416 $cm^2\ g^{-1}$. The findings show that the CL and the C have similar MAC values. This finding is remarkable because lead is usually a more effective radiation-shielding material than PDMS. The low density of PDMS, which affects the MAC calculation, causes the similarity in MAC values. Tin offers significant attenuation even though it is less effective than lead, according to CT, which has a MAC of 0.0916 $cm^2\ g^{-1}$ and a LAC of 0.6680 cm^{-1}. Because lead has a larger atomic number, which improves photon interaction, CL has a greater LAC than CT.

PT1 (10% tin) had the lowest MAC of 0.0470 $cm^2\ g^{-1}$ and LAC of 0.0754 cm^{-1} in tin-reinforced PDMS composites, indicating that a low tin concentration does not considerably enhance shielding. Among the tin-based composites, PT5 (0.0905 $cm^2\ g^{-1}$ MAC, 0.3622 cm^{-1} LAC) and PT6 (0.0762 $cm^2\ g^{-1}$ MAC, 0.3427 cm^{-1} LAC) had the greatest LAC values. Both MAC and LAC improve as the tin concentration rises. Due to tin's larger density and atomic number, which improve photon absorption, attenuation has increased. With a MAC of 0.0607 $cm^2\ g^{-1}$

International Journal of Innovation and Industrial Revolution
IJIREV
EISSN: 2637-0972
Volume 7 Issue 20 (March 2025) PP. 352-369
DOI 10.35631/IJIREV.720023

and an LAC of 0.2062 cm^{-1}, PT4 offers excellent shielding efficiency while balancing attenuation performance and material composition. The HVL and MAC for all composite samples is displayed in Figure 7. The thickness of a substance required to decrease radiation intensity by half (50%) of its original value is known as the HVL. Better shielding efficiency is indicated by a lower HVL.

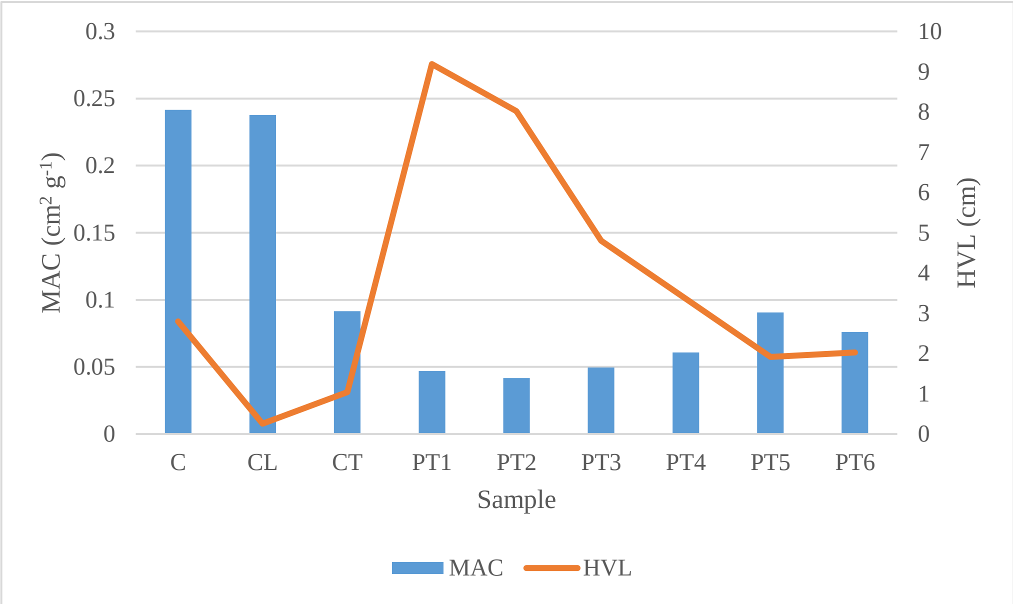

Figure 7: HVL Values of C, CL, CT, and PT Composites Against MAC at 356 KeV Energy Level

Lead-reinforced composite has greater attenuation qualities, as evidenced by the fact that CL's HVL is much lower than that of other composites. Because lead has a high atomic number, which increases photoelectric absorption and makes it a very effective radiation shielding material, a lower HVL in CL is to be expected. Conversely, CT, which stands for the tin-based control composite, has a much greater HVL but a lower MAC than C and CL. According to this, tin is less effective than lead but offers a moderate attenuation. Poor shielding performance at low tin concentrations is indicated by PT1 and PT2, the tin-reinforced PDMS composites with the highest HVL and the lowest MAC values.

Better radiation shielding capabilities are indicated by improved MAC values and decreased HVL as the tin content in PT3 to PT6 rises. With higher MAC and lower HVL, PT5 and PT6 notably show the best balance, indicating improved photon attenuation. These findings suggest that although lead is still the most efficient shielding material, PDMS composites' shielding capacity is greatly enhanced by adding tin, which makes PT5 and PT6 attractive options for long-term radiation shielding applications.

HVL, TVL, MFP and RPE values in Table 5 provide additional information about the composites' ability to protect against radiation. The thickness of a substance required to lower radiation intensity to a tenth (10%) of its initial value is known as the TVL. The average distance a photon travels through a substance before coming into contact with an atom is known as the MFP. Better attenuation results from more frequent interaction, which is suggested by a shorter MFP.

International Journal of Innovation and Industrial Revolution
EISSN: 2637-0972
Volume 7 Issue 20 (March 2025) PP. 352-369
DOI 10.35631/IJIREV.720023

With a low RPE of 11.65% and the highest HVL (2.80 cm), TVL (9.30 cm), and MFP (4.14 cm), C is confirmed to have poor shielding qualities. On the other hand, CL shows the lowest TVL (0.85 cm) and HVL (0.26 cm), indicating the greater attenuation efficiency of lead. Lead's large atomic number and density, which improve photon absorption, also contribute to its RPE of 74.01%, which is noticeably greater than that of other samples.

Table 5: HVL, TVL, MFP, and RPE of the Prepared Tin/PDMS Composite Samples at 356 KeV of γ-ray Photon

Sample	HVL (cm)	TVL (cm)	MFP (cm)	RPE
C	2.80	9.30	4.14	11.65
CL	0.26	0.85	4.21	74.01
CT	1.04	3.45	10.91	28.40
PT1	9.19	30.52	21.30	3.41
PT2	8.02	26.65	23.91	4.39
PT3	4.80	15.94	20.18	7.24
PT4	3.36	11.17	16.47	9.98
PT5	1.91	6.36	11.04	16.26
PT6	2.02	6.72	13.13	16.89

With an HVL of 1.0376 cm, TVL of 3.45 cm, and MFP of 10.91 cm, CT is less effective than lead but exhibits superior attenuation than pure PDMS. Although tin's RPE of 28.39% indicates that metal offers moderate shielding qualities, lead outperforms it in terms of efficacy. With the lowest RPE values (3.41% and 4.39%), PT1 and PT2 exhibit the highest HVL (9.19 cm and 8.02 cm, respectively) and TVL (30.52 cm and 26.65 cm) among the tin-reinforced PDMS composites, suggesting that a lower tin content does not affect radiation shielding.

PT3 to PT6 show better attenuation characteristics as the tin compositions rise. While PT6 displays comparable data with an HVL of 2.02 cm and RPE of 16.89%, PT5 has an HVL of 1.91 cm, TVL of 6.36 cm, and MFP of 11.04 cm with an RPE of 16.26%. These findings imply that increased photon interactions decreased HVL and TVL values, and improved RPE are all indications that higher tin concentrations improve shielding. As anticipated, CL continues to be the best shielding material overall, but among tin-based composites, PT5 and PT6 show the most promising performance. Their potential as substitute radiation shielding materials with less of an adverse effect on the environment is shown by their enhanced attenuation qualities.

Conclusion

This study evaluated the radiation shielding properties of PDMS composites enhanced with tin as a potential replacement for Pb-based materials. The results demonstrated that CL had the highest MAC and the lowest HVL, confirming its superior shielding capacity. However, because of the health and environmental hazards associated with lead, alternative metals like tin-based composites were investigated.

FTIR analysis confirmed the structural stability of the PDMS matrix after tin reinforcement, with characteristic peaks indicating an effective bond between the polymer and the metal filler. An increase in tin content was associated with improved radiation attenuation, as seen by the tin-reinforced composites' higher MAC values and lower HVL. The most promising shielding performance was shown by PT5 and PT6, which balanced attenuation efficiency with material stability.

International Journal of Innovation and Industrial Revolution
EISSN: 2637-0972
Volume 7 Issue 20 (March 2025) PP. 352-369
DOI 10.35631/IJIREV.720023

The potential of tin-reinforced PDMS as a sustainable alternative for radiation shielding applications is demonstrated by this study. Future studies should focus on enhancing tin dispersion within the polymer matrix to further enhance attenuation efficiency, mechanical durability, and overall performance. These findings contributed to the development of Pb-free shielding materials, providing more effective and environmentally friendly radiation protection solutions.

Acknowledgement
The authors express their gratitude to the Ministry of Higher Education (MOHE) through the Fundamental Research Grant Scheme (FRGS/1/2023/STG05/UITM/03/3) for providing financial support. Also acknowledged were Universiti Teknologi MARA Cawangan Pulau Pinang, Universiti Putra Malaysia and Universiti Kebangsaan Malaysia, which gave access to workstation facilities and beneficial assistance.

References

Abualroos, N. J., Idris, M. I., Ibrahim, H., Kamaruzaman, M. I., & Zainon, R. (2024). Physical, mechanical, and microstructural characterisation of tungsten carbide-based polymeric composites for radiation shielding application. *Scientific Reports*, 14(1). Retrieved from https://doi.org/10.1038/s41598-023-49842-3

Aim-O, P., Wongsawaeng, D., Phruksarojanakun, P., & Tancharakorn, S. (2017). Monte carlo simulation of innovative neutron and photon shielding material composing of high density concrete, waste rubber, lead and boron carbide. *Journal of Physics: Conference Series*, 860(1). Retrieved from https://doi.org/10.1088/1742-6596/860/1/012043

Aladailah, M. W., Tashlykov, O. L., Volozheninov, T. P., Kaskov, D. O., Iuzbashieva, K. S., Al-Abed, R., … Alshipli, M. (2022). Exploration of physical and optical properties of ZnO nanopowders filled with polydimethylsiloxane (PDMS) for radiation shielding applications. Simulation and theoretical study. *Optical Materials*, 134, 113197. Retrieved 23 October 2024 from https://doi.org/10.1016/j.optmat.2022.113197

Ali, Y. F., Cucinotta, F. A., Ning-Ang, L., & Zhou, G. (2020). Cancer risk of low dose ionizing radiation. *Frontiers in Physics*, 8, 1–9. Retrieved from https://doi.org/10.3389/fphy.2020.00234

Alresheedi, M. T., Elsafi, M., Aladadi, Y. T., Abas, A. F., Ganam, A. Bin, Sayyed, M. I., & Mahdi, M. A. (2023a). Assessment of silicone rubber / Lead oxide composites. *Polymers*, 15(9). Retrieved 24 January 2024 from https://doi.org/https://doi.org/10.3390/polym15092160

Alresheedi, M. T., Elsafi, M., Aladadi, Y. T., Abas, A. F., Ganam, A. Bin, Sayyed, M. I., & Mahdi, M. A. (2023b). Assessment of Silicone Rubber/Lead Oxide Composites Enriched with Bi2O3, WO3, BaO, and SnO2 Nanoparticles for Radiation Shielding Applications. *Polymers*, 15(9). Retrieved from https://doi.org/10.3390/polym15092160

Alshahri, S., Alsuhybani, M., Alosime, E., Alotaibi, S., Almurayshid, M., & Alrwais, A. (2021). Ldpe/bismuth oxide nanocomposite: Preparation, characterization and application in x-ray shielding. *Polymers*, 13(18). Retrieved from https://doi.org/10.3390/polym13183081

Altan, M., & Yavuz, B. (2016). Novel method for manufacturing polymer/metal hybrid structures. *Acta Physica Polonica A*, 129(4), 639–641. Retrieved from https://doi.org/10.12693/APhysPolA.129.639

Asgari, M., Afarideh, H., Ghafoorifard, H., & Amirabadi, E. A. (2021). Comparison of nano/micro lead, bismuth and tungsten on the gamma shielding properties of the

International Journal of Innovation and Industrial Revolution
IJIREV
EISSN: 2637-0972
Volume 7 Issue 20 (March 2025) PP. 352-369
DOI 10.35631/IJIREV.720023
flexible composites against photon in wide energy range (40 keV–662 keV). *Nuclear Engineering and Technology*, 53(12), 4142–4149. Retrieved from https://doi.org/10.1016/j.net.2021.06.022

Barabash, A., Barabash, D., Pertsev, V., & Panfilov, D. (2019). Polymer-composite materials for radiation protection. *Advances in Intelligent Systems and Computing*, 983, 352–360. Retrieved from https://doi.org/10.1007/978-3-030-19868-8_36

Bijanu, A., Arya, R., Agrawal, V., Tomar, A. S., Gowri, V. S., Sanghi, S. K., … Salammal, S. T. (2021, October 1). Metal-polymer composites for radiation protection: a review. *Journal of Polymer Research*. Springer Science and Business Media B.V. Retrieved from https://doi.org/10.1007/s10965-021-02751-3

Boniface, I. J., & Mukhtar, N. M. A. (2020). A study on the importance of personal protective equipment (PPE) in occupational radiation protection. 9th Virtual Science Invention Conference (SIIC) 2020.

Cioffi, D. L., Fontana, L., Leso, V., Dolce, P., Vitale, R., Vetrani, I., … Iavicoli, I. (2020). Low dose ionizing radiation exposure and risk of thyroid functional alterations in healthcare workers. *European Journal of Radiology*, 132, 109279. Retrieved from https://doi.org/10.1016/j.ejrad.2020.109279

El-Khatib, A. M., Abbas, M. I., Elzaher, M. A., Badawi, M. S., Alabsy, M. T., Alharshan, G. A., & Aloraini, D. A. (2019). Gamma attenuation coefficients of nano cadmium oxide/high density polyethylene composites. *Scientific Reports*, 9(1), 1–11. Retrieved from https://doi.org/10.1038/s41598-019-52220-7

Ersoz, O. A., Lambrecht, F. Y., & Soylu, H. M. (2016). Tungsten-ethylene vinyl acetate (EVA) composite as a gamma rays shielding material. *Indian Journal of Pure and Applied Physics*, 54(12), 793–796.

Gouda, M. M., Abbas, M. I., Hammoury, S. I., Zard, K., & El-Khatib, M. A. (2023). Nano tin oxide/dimethyl polysiloxane reinforced composite as a flexible radiation protecting material. *Scientific Reports*, 13(1), 1–13. Retrieved from https://doi.org/10.1038/s41598-023-27464-z

Kamarolzeman, J. A., & Mukhtar, N. M. A. (2020). A review on the personal protective equipment (PPE) used in occupational radiation protection. 9th Virtual Science Invention Innovation Conference (SIIC) 2020.

Kaur, T., Sharma, J., & Singh, T. (2019). Review on scope of metallic alloys in gamma rays shield designing. *Progress in Nuclear Energy*, 113(April 2018), 95–113. Retrieved from https://doi.org/10.1016/j.pnucene.2019.01.016

Kawady, N. A., Elkattan, M., Salah, M., & Galhoum, A. A. (2022). Fabrication, characterization, and gamma ray shielding properties of PVA-based polymer nanocomposite. *Journal of Materials Science*, 57(24), 11046–11061. Retrieved from https://doi.org/10.1007/s10853-022-07213-9

Kilicoglu, O., More, C. V., Akman, F., Dilsiz, K., Oğul, H., Kaçal, M. R., … Agar, O. (2022). Micro Pb filled polymer composites: Theoretical, experimental and simulation results for γ-ray shielding performance. *Radiation Physics and Chemistry*, 194. Retrieved from https://doi.org/10.1016/j.radphyschem.2022.110039

Kochanova, D., Gulati, S., Durdik, M., Jakl, L., Kosik, P., Skorvaga, M., … Belyaev, I. (2023). Effects of low-dose ionizing radiation on genomic instability in interventional radiology workers. *Scientific Reports*, 13(1), 1–11. Retrieved from https://doi.org/10.1038/s41598-023-42139-5

Körpınar, B., Öztürk, B. C., Çam, N. F., & Akat, H. (2020). Investigations on thermal and radiation shielding properties of the poly(hydroxyethyl methacrylate-co-

International Journal of Innovation and Industrial Revolution
EISSN: 2637-0972
IJIREV
Volume 7 Issue 20 (March 2025) PP. 352-369
DOI 10.35631/IJIREV.720023

styrene)/tungsten(VI) oxide composites. *Progress in Nuclear Energy*, 126. Retrieved from https://doi.org/10.1016/j.pnucene.2020.103424

M. El-Sharkawy, R., Abdou, F. S., Gizawy, M. A., Allam, E. A., & Mahmoud, M. E. (2023). Bismuth oxide nanoparticles (Bi2O3 NPs) embedded into recycled- Poly(vinyl chloride) plastic sheets as a promising shielding material for gamma radiation. *Radiation Physics and Chemistry*, 208, 110838. Retrieved from https://doi.org/10.1016/j.radphyschem.2023.110838

Mehrara, R., Malekie, S., Kotahi, S. M. S., & Kashian, S. (2021). Introducing a novel low energy gamma ray shield utilizing Polycarbonate Bismuth Oxide composite. *Scientific Reports*, 11(1), 1–13. Retrieved from https://doi.org/10.1038/s41598-021-89773-5

Mollah, A. S. (2019). Evaluation of Gamma Radiation Attenuation Characteristics of Different Type Shielding Materials used in Nuclear Medicine Services. *Bangladesh Journal of Nuclear Medicine*, 21(2), 108–114. Retrieved from https://doi.org/10.3329/bjnm.v21i2.40361

Mukhtar, N. M. A., Mahmood, A., Suhaimi, A. N., Noor Azman, N. F. H., Kamarolzeman, J. A., Boniface, I. J., & Safian, A. (2024). The effects of education level on radiation professionals' knowledge and implementation of ALARA principles for occupational radiation protection. *Journal of Islamic, Social, Economics, and Development (JISED)*, 9(60), 82–92. Retrieved from 10.55573/JISED.096010

Ozel, F., Akman, F., Kaçal, M. R., Ozen, A., Arslan, H., Polat, H., … Agar, O. (2021). Production of microstructured BaZrO3 and Ba2P2O7-based polymer shields for protection against ionizing photons. *Journal of Physics and Chemistry of Solids*, 158, 110238. Retrieved from https://doi.org/10.1016/j.jpcs.2021.110238

Pianpanit, T., & Saenboonruang, K. (2022). High-energy photon attenuation properties of lead-free and self-healing poly (vinyl alcohol) (PVA) hydrogels: numerical determination and simulation. *Gels*, 8(4). Retrieved from https://doi.org/10.3390/gels8040197

Rajendran, S., Palani, G., Kanakaraj, A., Shanmugam, V., Veerasimman, A., Gądek, S., … Marimuthu, U. (2023). Metal and polymer based composites manufactured using additive manufacturing—a brief review. *Polymers*, 15(11), 1–19. Retrieved from https://doi.org/10.3390/polym15112564

Vaiserman, A., Koliada, A., Zabuga, O., & Socol, Y. (2018). Health impacts of low-dose ionizing radiation: current scientific debates and regulatory issues. *Dose-Response*, 16(3), 1–27. Retrieved from https://doi.org/10.1177/1559325818796331

Wahyuni, F., Sakti, S. P., Herry Santjojo, D. J. D., & Juswono, U. P. (2022). Bismuth oxide filled polyester composites for X-ray radiation shielding applications. *Polish Journal of Environmental Studies*, 31(4), 3985–3990. Retrieved from https://doi.org/10.15244/pjoes/146935

Wang, J., Zhou, H., Gao, Y., Xie, Y., Zhang, J., Hu, Y., … Mi, A. (2021). The characterization of silicone-tungsten-based composites as flexible gamma-ray shields. *Materials*, 14(20). Retrieved from https://doi.org/10.3390/ma14205970

Yılmaz, S. N., Güngör, A., & Özdemir, T. (2020). The investigations of mechanical, thermal and rheological properties of polydimethylsiloxane/bismuth (III) oxide composite for X/Gamma ray shielding. *Radiation Physics and Chemistry*, 170, 108649. Retrieved 4 February 2025 from https://doi.org/10.1016/J.RADPHYSCHEM.2019.108649

Zainal Abidin, H., Mukhtar, N. M. A., Mahmood, A., Abdul Wahab, N. A., Zainon, R., Roslan, N. S., … Zarzali Shah, A. (2025). Effect of tin filler composition on porosity in tin-polydimethylsiloxane composites. *Pure and Applied Chemistry*. Retrieved 10 April 2025 from https://doi.org/10.1515/PAC-2024-0347

Volume 7 Issue 20 (March 2025) PP. 352-369
DOI 10.35631/IJIREV.720023
Zhang, Y. J., Guo, X. T., Wang, C. H., Lu, X. A., Wu, D. F., & Zhang, M. (2021). Gadolinium- and lead-containing functional terpolymers for low energy X-ray protection. *Nuclear Engineering and Technology*, 53(12), 4130–4136. Retrieved from https://doi.org/10.1016/j.net.2021.06.021